J Fluoresc (2016) 26:1279–1293
DOI 10.1007/s10895-016-1815-2

ORIGINAL ARTICLE

Red Emitting Coumarin—Azo Dyes : Synthesis, Characterization, Linear and Non-linear Optical Properties-Experimental and Computational Approach

Abhinav B. Tathe[1] · **Nagaiyan Sekar**[1]

Received: 13 December 2015 / Accepted: 26 April 2016 / Published online: 7 May 2016

Abstract The coumarin molecules with 7-(N,N-diethylamino) substitution and aryl azo (Ar–N=N-) at 3-position were synthesized, by reacting diazonium salt of substituted amines and 7-(N, N-diethylamino)-4-hydroxy coumarin under basic conditions. They were found to be fluorescent despite the presence of azo group. The azo group rotation was blocked by complexing with -BF_2, so as to get a red shift in absorption. The azo molecules show charge transfer, whereas BF_2-complexes do not. The dipole moment ratios between the ground and excited states calculated suggest highly polar excited state and an intra-molecular charge transfer at the excited state in the case of azo dyes. The NLO properties were calculated by solvatochromic method and computationally. Second order hyperpolarizability was found to be 46 to 1083 times more than urea. DFT and TDTDF calculations were performed to understand the electronic properties of the molecules at the ground as well as excited states.

Keywords Azo dye · Coumarin · Red emitting · DFT · TDDFT · NLO properties

Electronic supplementary material The online version of this article (doi:10.1007/s10895-016-1815-2) contains supplementary material, which is available to authorized users.

✉ Nagaiyan Sekar
n.sekar@ictmumbai.edu.in; nethi.sekar@gmail.com

[1] Tinctorial Chemistry Group, Institute of Chemical Technology, N. P. Marg, Matunga, Mumbai 400 019, India

Introduction

Many of the known coumarins are fluorescent molecules and they are known to have good quantum yield [1, 2] and high photostability [3, 4]. Most of the them are colorless but substitutions at various positions bring about a red shift in absorption and emission, and are used in the applications such as laser dyes [5], textile dyes [6] and sensors [7]. Coumarins have also been used as optical brighteners [8], non-linear optical (NLO) materials [9] and in biological labelling [10, 11]. The compounds with azo functionality are less fluorescent to non-fluorescent in nature. Azo functional group at the 3-position of 4-hydroxy coumarin molecule was first reported by Yazdanbaksh et al. [12]. In the later studies on these molecules UV–vis absorption, fluorescence and acid dissociation constants were reported [12, 13]. The substituent at 7-position plays an important role in the photophysical properties of coumarins [14, 15] and imparts a red shift in absorption if the 7-substituent happens to be electron releasing. Here we report the synthesis of four 7-(N,N-diethylamino)-3-azo coumarin dyes with different substitutions at the 4-position of the phenylazo core (Fig. 2). The properties like absorption, emission and quantum yield are studied. The dominant tautomer among the azo and hydrazine (Fig. 2) form is established by DFT. The effect of rigidization of azo functional with BF_2-complexation is also studied in comparison with the parent molecules. The rigidization of the azo group is known with N-B-N=N kind of bridge [16, 17] and no much information is given on O-B-N=N type of bridge particularly in an azo coumarin system. This happens to be the first study of this kind. The N-B-N=N bridge has introduced the red shifts in the absorption characteristics of the molecules [17] (Fig. 1). The red shift in the molecule was attributed to the azo rigidization and the resulting π-resonance effect (Fig. 2).

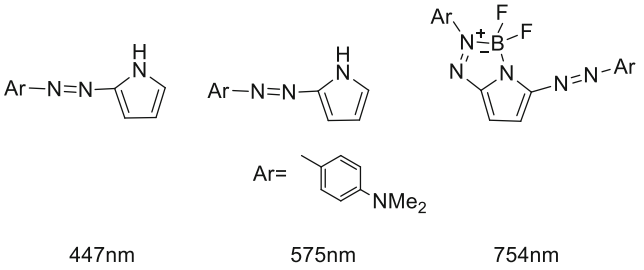

Fig. 1 Azo rigidization

The photophysical behavior of these molecules was probed for sensitivity towards solvent polarity. DFT calculations were used to get insights into the photophysical properties.

Experimental

Materials and Equipments

All the commercial reagents were procured from SD Fine Chemicals (Mumbai) and were used without further purification. Laboratory reagent grade solvents were purchased from Rankem, Mumbai. The reactions were monitored by TLC using 0.25 mm E-Merck silica gel 60 F_{254} precoated plates, which were visualized with UV light (254 and 344 nm). Melting points were measured on standard melting point apparatus from Sunder Industrial products Mumbai and are uncorrected. ^{1}HNMR spectra were recorded on Bruker 400 MHz and Agilent 500 MHz instruments using TMS as an internal standard. Mass spectra were recorded on FINNIGAN LCQ ADVANTAGE MAX instrument from Thermo Electron Corporation (USA). The absorption spectra of the compounds were recorded on a Perkin Elmer Lambda 25 UV-Visible spectrophotometer; Emission spectra were recorded on Varian Inc. Cary Eclipse spectrofluorometer.

The ground state (S_0) geometries of the tautomers of the compounds **3a-3d** were optimized in the gas phase using Density Functional Theory (DFT) [18]. The popular hybrid functional B3LYP was used, which combines Becke's three parameter exchange functional (B3) [19] with the nonlocal correlation functional by Lee, Yang, and Parr (LYP) [20]. All the atoms were treated with 6–31 G(d) basis set, which deems to be sufficient for the type of molecules involved [21–23]. The validity of the structures as local minima on potential energy surface was verified with vibrational analysis and confirmed that they are with no imaginary frequencies. Time Dependent Density Functional Theory (TD-DFT) with the same hybrid functional and basis set was used to estimate vertical excitations and oscillator strengths . The lowest singlet excited state (S_1) was relaxed using TD-DFT to get optimised geometry of the excited state. The vertical emissions were computed by using the optimized relaxed singlet first excited state (S_1). Frequency computations were carried out on the optimized geometry of the low-lying vibronically relaxed first excited state of the conformers. All the computations in solvents were carried out using the Polarizable Continuum Model (PCM) [24].

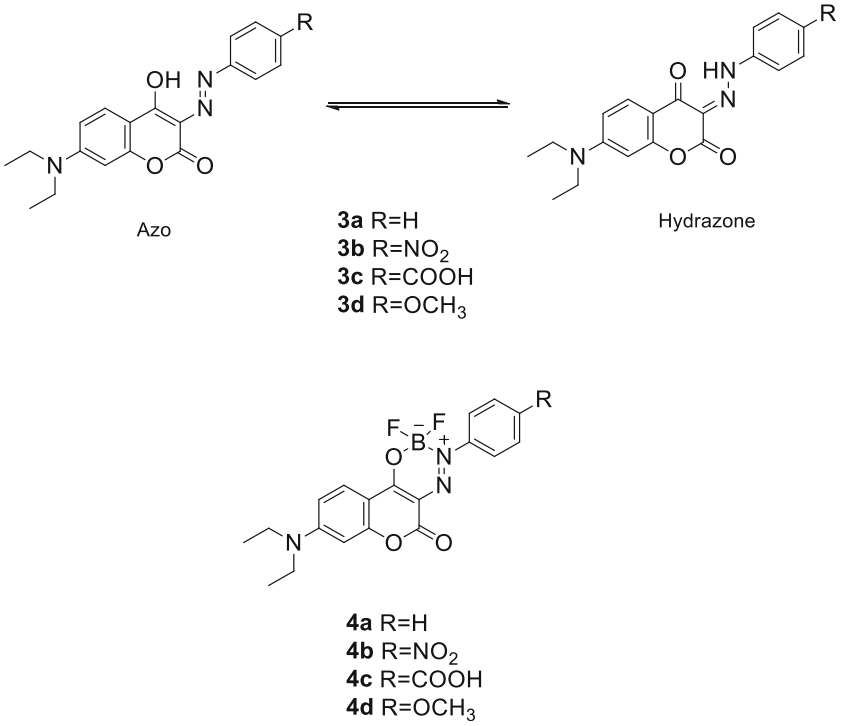

Fig. 2 7-(N,N-diethylamino) 3-azo coumarin dyes (azo and hydrazone form) and their BF_2-Complexes

Gaussian 09 program [25] was used for all the DFT and TDDFT computations and the results were visualized with Gauss View 5.0 [26].

Synthesis and Characterization

The compound **1** was synthesized by the method reported [27] from bis(2,4-dichlorophenyl) malonate and 3-(diethylamino)phenol. The product obtained was sufficiently pure to be used for the further steps.

General Procedure for Diazotization and Coupling

Substituted aniline (2.5 mmol) was dissolved in 11 N hydrochloric acid (3 mL) and was cooled externally to −5 °C in ice-salt mixture. A solution of sodium nitrite (0.22 g, 3.1 mmol) in 1 ml water was added to the above dropwise with stirring. The solution thus formed was then stirred for 1 h at the same temperature. Excess nitrous acid was quenched with the addition of urea (1.5 mmol) to this solution. In an another flask 7-(diethylamino)-4-hydroxy-2H-chromen-2-one (0.5 g, 2.1 mmol) was dissolved in pre-cooled 5 % NaOH solution (5 mL) which was then placed in an ice-salt bath, and the diazonium salt prepared in the first flask was slowly added maintaining the pH 8–9 with the addition of solid sodium carbonate. After complete addition the reaction mixture was stirred for a period of 1 h and then neutralized with dilute hydrochloric acid. The yellow to brick red precipitate formed was then filtered, washed with water and dried under vacuum to give the product in good yield (Fig. 3).

7-(Diethylamino)-4-hydroxy-3-(phenyldiazenyl)-2H-chromen-2-one (3a)

Yield: 80 %

M.P.: 190 °C

^{1}HNMR ($CDCl_3$, 400 MHz) **:δ** 1.24 (t, J=7.2Hz, 6H), 3.45 (q, J=7.2Hz, 4H), 6.35 (s, 1H), 6.57 (m, 1H), 7.23 (s, 1H), 7.42 (t, J=8Hz, 2H), 7.59 (d, J=8Hz, 2H), 7.85 (d, J=8Hz, 2H).

HRMS : 338.1480 (M+1) (Calculated for **$C_{19}H_{20}N_3O_3$**: 338.1426)

^{13}CNMR (DMSO-d_6, 125 MHz): δ 12.9, 44.7, 97.3, 109.4, 114.18, 118.3, 125.81, 128.36, 144.5, 156.3, 158.5, 162.21, 164.3.

7-(Diethylamino)-4-hydroxy-3-((4-nitrophenyl)diazenyl)-2H-chromen-2-one (3b)

Yield: 85 %

M.P.: 260 °C

^{1}HNMR ($CDCl_3$, 400 MHz) **:δ** 1.26 (t, J=7.2Hz, 6H), 3.48 (q, J=7.2Hz, 4H), 6.36 (d, J=2.4Hz, 1H), 6.60 (dd, J=6.4 & 2.4Hz, 1H), 7.67 (d, J=9.2Hz, 2H), 7.86 (d, J=6.4 Hz, 1H), 8.31 (d, J=9.2Hz, 2H)

HRMS: 383.1319 (M+1) (Calculated for **$C_{19}H_{19}N_4O_5$**: 383.1355)

^{13}CNMR (DMSO-d_6, 125 MHz): 12.9, 51.6, 96.9, 109.5, 117.4, 122.5, 126.3, 128.7, 130.1, 154.0, 156.7, 159.1.

4-((7-(Diethylamino)-4-hydroxy-2-oxo-2H-chromen-3-yl)diazenyl)benzoic acid (3c).

After acidifying the solution remained clear and was saturated with sodium chloride to give brick red coloured precipitate.

Yield: 68 %

M.P.: >300 °C

^{1}HNMR ($CDCl_3$, 400 MHz) **:δ** 1.25 (t, J=7.2Hz, 6H), 3.45(q, 6H), 6.34(s, 1H), 6.58(d, J=6Hz, 1H), 7.63(d, J=8.6Hz, 2H), 7.88 (d, J=6Hz, 1H), 8.14 (d, J=8.6Hz, 2H).

HRMS : 382.1375 (M+1) (Calculated for **$C_{20}H_{20}N_3O_5$**: 382.1403)

^{13}CNMR (DMSO-d_6, 125 MHz): δ 12.7, 44.4, 97.3, 109.7, 116.906, 123.9, 128.4, 131.2, 154.0, 156.3, 158.8, 167.1, 176.8.

7-(Diethylamino)-4-hydroxy-3-((4-methoxyphenyl)diazenyl)-2H-chromen-2-one (3d)

Yield: 82 %

M.P.: 205 °C

^{1}HNMR ($CDCl_3$, 400 MHz) **:** δ 1.24(t, 6H), 3.45(q, 4H), 3.89(s, 3H), 6.37(d, J=2.4Hz, 1H), 6.58(dd, J=6.4&2.4Hz, 1H), 6.96(d, J=8.8Hz, 2H), 7.56(d, J=8.8Hz, 2H), 7.85(d, J=6.4Hz, 1H)

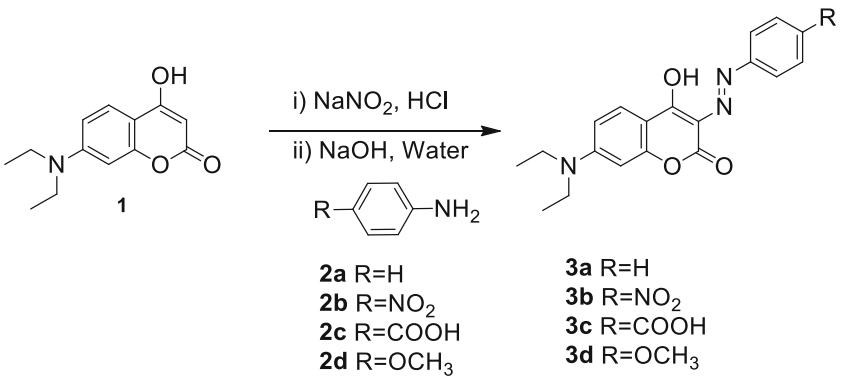

Fig. 3 Synthesis of 7-(N,N-diethylamino)-4-hydroxy 3-azo coumarin dyes

HRMS: 368.1590 (M+1) (Calculated for $C_{20}H_{22}N_3O_4$: 368.1610)

^{13}CNMR (DMSO-d_6, 125 MHz): δ 11.9, 44.4, 54.5, 96.9, 108.0, 114.9, 119.0, 121.8, 123.2, 129.1, 134.6, 153.9, 156.3, 159.467, 176.1

General Procedure for BF_2-complexation

The azo compound (**3a-3d**) (1 mmol) was dissolved in 20 mL of dry acetonitrile. To this solution, BF_3-Et_2O solution (45–50 % solution, 2 mL) was added dropwise. The resultant solution was stirred and refluxed under nitrogen environment. After completion of the reaction, the mixture was cooled and the dark colored precipitate formed was filtered, washed with diethyl ether (20 mL) and dried under vacuum (Fig. 4).

8-(Diethylamino)-2,2-difluoro-5-oxo-3-phenyl-2,5-dihydrochromeno[3,4-e][1,3,4,2]oxadiaza borinin-3-ium-2-uide (4a)

Yield: 70 %

M.P.: 272 °C

^{1}HNMR ($CDCl_3$, 500 MHz) **:** δ 1.30(t, 3H), 3.54(q, 4H), 6.46(s, 1H), 6.71(d, *J*=10Hz, 1H), 7.45(m, 3H), 7.96(t, *J*=8.5Hz, 3H).

HRMS: 386.1464 (M+1) (Calculated for $C_{19}H_{19}BF_2N_3O_3$: 386.1488)

^{13}CNMR (DMSO-d_6, 125 MHz): δ 12.5, 45.7, 97.35, 110.93, 122.0, 129.2, 129.5, 129.7, 155.9, 157.7, 159.8.

8-(Diethylamino)-2,2-difluoro-3-(4-nitrophenyl)-5-oxo-2,5-dihydrochromeno[3,4-e][1,3,4,2] oxadiazaborinin-3-ium-2-uide (4b)

Yield: 82 %

M.P.: 270 (dec.)°C

^{1}HNMR ($CDCl_3$, 500 MHz)**:** δ 1.33(t, *J*=7.5Hz, 6H), 3.59(q, *J*=7.5Hz, 4H), 6.47(d, *J*=2.5Hz, 1H), 6.74(d,d, *J*=2.5,5.5Hz, 1H), 7.98(d, *J*=10Hz, 1H), 8.12(d,J=10Hz, 2H), 8.31(d, *J*=9.5Hz, 2H).

HRMS: 431.1318 (M+1) (Calculated for $C_{19}H_{18}BF_2N_4O_5$:431.1338)

^{13}CNMR (DMSO-d_6, 125 MHz): δ 12.6, 46.1, 97.7, 111.6, 122.0, 124.8, 125.7, 130.3, 156.7, 159.24.

3-(4-Carboxyphenyl)-8-(diethylamino)-2,2-difluoro-5-oxo-2,5-dihydrochromeno[3,4-e][1,3,4,2] oxadiaza borinin-3-ium-2-uide (4c)

Yield: 50 %

M.P.: 200 °C

^{1}HNMR ($CDCl_3$, 500 MHz) **:** δ 0.90(t, *J*=7.5Hz, 6H), 3.24(q, *J*=7.5Hz, 4H), 6.16(d, *J*=2.5Hz, 1H), 6.44(q, *J*=4Hz, 1H), 7.48(d, *J*=4Hz, 1H), 7.59(q, *J*=3.5Hz), 7.74(d,d, *J*=5Hz,3.5Hz, 2H).

HRMS: 430.1355 (M+1) (Calculated for $C_{20}H_{19}BF_2N_3O_5$: 430.1386)

^{13}CNMR (DMSO-d_6, 125 MHz): δ 176.1, 167.1, 158.5, 156.3, 153.9, 144.3, 130.1, 129.7, 128.3, 127.65, 123.6, 120.8, 117.0, 109.7, 108.3, 101.4, 97.6, 96.6, 44.4, 12.9.

8-(Diethylamino)-2,2-difluoro-3-(4-methoxyphenyl)-5-oxo-2,5-dihydrochromeno[3,4-e][1,3,4,2] oxadiazaborinin-3-ium-2-uide (4d)

Yield: 85 %

M.P.: 205 °C

^{1}HNMR ($CDCl_3$, 500 MHz) **:** δ 1.30(t, *J*=7.5Hz, 6H), 3.53(q, *J*=7.5Hz, 4H), 3.88(s, 3H), 6.45(d, *J*=10Hz, 1H), 6.69(q, *J*=5Hz, 1H), 6.97(q, *J*=10Hz, 1H), 7.93(d, *J*=5Hz, 1H), 7.96(m, 3H).

HRMS: 416.1585 (M+1) (Calculated for $C_{20}H_{21}BF_2N_3O_4$: 416.1593)

^{13}CNMR (DMSO-d_6, 125 MHz): δ 12.5, 45.6, 55.6, 97.3, 110.7, 110.7, 114.4, 114.9, 123.6, 128.3, 129.12, 155.5, 158.4, 161.1.

Result and Discussion

Structural Properties of Compound 3a-3d and 4a-4d

The geometries of the compounds **3a-3d** were optimised in solvent environments using DFT. These kind of dyes are known to exhibit azo-hydrazone tautomerism [28–30]. Therefore both the forms i.e. azo and hydrazone tautomers (Fig. 2) were optimised with DFT-B3LYP/6-31 g(d). The comparison of the energy values of azo (enol form) and hydrazone (keto form) has revealed that the latter is more

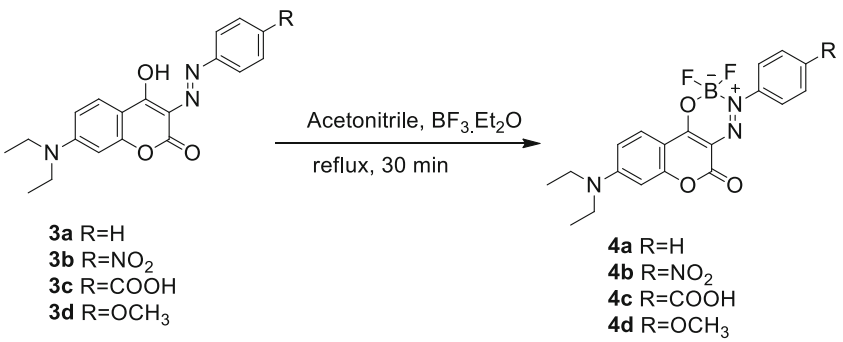

Fig. 4 BF_2-Complexation of 7-(N,N-diethylamino)-4-hydroxy 3-azo coumarin dyes

stable in terms of total energy of the optimised structures (Supporting information). The hydrazone structure is used for further optimizations and calculation of the electronic properties. The energy values also has revealed that the substituent effect is also important to the stabilisation energy as the $–NO_2$ substituted compound **3b** is the most stable and the unsubstituted one i.e. compound **3a** is the least stabilised. The stabilities of the compounds **3c** and **3d** is intermediate. Among these the electron withdrawing group –COOH in the compound **3c** has enhanced the molecular stability as compared the $–OCH_3$ of the compound **3d**. The bond length and dihedral angle analysis suggests that, O-atom of keto functional group in hydrazone form in the compounds **3a-3d** shows H-bonding with the hydrogen on the =N-N-H. This suggests that the molecules may be in tautomeric equilibrium in solutions.

Linear Optical Properties

The compounds were studied for their photophysical properties in solvents of various polarity and nature. The absorption properties of the compounds **3a-3d** are summarised in Table 1.

The absorption properties in terms of absorption wavelength are not much sensitive towards solvent polarity. The

Table 1 Photophysical properties of compound **3a-3d** and comparison with theoretical values

	Solvent	Experimental					Theoretical[a]		
		λ_{abs} (nm)	*f*	λ_{em} (nm)	Stokes shift (cm^{-1})	Φ	Vertical excitation (nm)	*f*	Emission (nm)
3a	ACN	460	0.512	622	5662	0.0028	459	0.740	557
	DCM	453	0.243	588	5068	0.0131	456	0.783	557
	DMF	461	0.736	611	5325	0.0024	461	0.766	581
	DMSO	460	0.478	–	–	–	461	0.761	–
	EtOAc	457	0.427	582	4700	0.0157	453	0.779	555
	EtOH	463	0.221	605	5069	0.0030	459	0.749	557
	MeOH	463	0.243	613	5285	0.0011	459	0.736	556
	Tol	456	0.354	539	3377	0.0094	446	0.857	552
3b	ACN	482	0.481	648	5315	0.0007	522	0.605	639
	DCM	485	0.492	623	4567	0.0039	516	0.645	637
	DMF	476	0.454	635	5260	0.0005	524	0.628	642
	DMSO	470	0.343	–	–	–	525	0.623	–
	EtOAc	475	0.468	617	4845	0.0032	511	0.643	634
	EtOH	480	0.447	606	4332	0.0007	521	0.613	639
	MeOH	478	0.492	646	5441	0.0003	522	0.602	639
	Tol	479	0.487	580	3635	0.0180	496	0.723	631
3c	ACN	471	0.272	634	5459	0.0013	482	0.733	592
	DCM	480	0.145	610	4440	0.021	479	0.774	593
	DMF	470	0.614	635	5529	0.0013	484	0.757	619
	DMSO	477	0.480	–	–	–	484	0.752	–
	EtOAc	466	0.370	602	4848	0.0079	475	0.771	591
	EtOH	475	0.393	606	4551	0.0014	482	0.741	593
	MeOH	473	0.145	613	4828	0.0013	482	0.729	592
	Tol	468	0.258	559	3478	0.0140	466	0.850	593
3d	ACN	474	0.644	604	4541	0.0039	466	1.039	535
	DCM	480	0.701	570	3289	0.0071	464	1.081	534
	DMF	477	0.600	608	4517	0.0037	468	1.065	538
	DMSO	477	0.289	–	–	–	468	1.060	–
	EtOAc	469	0.582	559	3433	0.0042	461	1.074	531
	EtOH	477	0.468	581	3753	0.0028	466	1.047	535
	MeOH	474	0.701	603	4513	0.0011	465	1.034	534
	Tol	472	0.549	534	2460	0.0023	456	1.133	537

[a] TD-B3LYP/6-31G(d)

FWHM (Full width at half maximum) values for all the dyes **3a-3d** are higher in polar aprotic solvents like N,N-dimethylformamide (DMF) and dimethylsulphoxide (DMSO) indicating broadening of the spectra in dipolar aprotic solvents. For the compound **3b** the values are higher in polar protic solvents also. The other molecules **3a**, **3c-3d** show lower FWHM values for the protic solvents. The polar aprotic solvents also shows higher integrated absorption coefficients (IAC) in all the dyes except in 3b. The values for the IAC falls in the range of $0.3357–1.7028 \times 10^{8}$. The molar extinction co-efficient at λ^{max} is the highest for the chlorinated non polar solvent dichloromethane (DCM). The observation is consistent with all the substituents. The absorption cross-section is also the highest in DCM, and has reached up to 2.01×10^{-19} cm^{-2} for the compound **3d**.

In an analogous manner the compounds **4a-4d** are less sensitive to the polarity but has different features in various solvents (Supporting Information). An increase of the FWHM is observed here for the polar protic solvents i.e. methanol and ethanol. Also there is two-fold increase in the molar absorptivity (ε^{max}) of the compounds **4a-4d** when compared with their counterparts in the compounds **3a-3d**. This is due to the lowering of HOMO-LUMO gap (longer wavelength absorption) and apparent increase in the concentration of the absorbing species. The IAC values are also higher than the values of the compounds **3a-3d**. Amongst all the BF_2-complexes **3a** and **3d** show an increase in absorption cross section. The oscillator strengths (f) are not sensitive to the polarities of the solvents and shows no clear correlation.

The compounds **4a-4d** are red shifted as against their parent azo compounds **3a-3d**. The FWHM values are also higher and a broader absorption is indicated. The molar extinction co-efficients of the azo-BF2 complexes are improved over the azo compounds. Absorption cross section values are in the range of $0.93–2.91 \times 10^{-19}$ cm^{-2} in all the solvents.

Absorption and Solvatochromism

The compounds **3a-3d** were studied for their solvatochromic properties in various solvents of different polarities. The absorption wavelengths were insensitive to solvent polarity (Table 1). The dyes **3a-3d** show the highest molar extinction coefficient in the solvent dichloromethane (DCM) (Table 1).

However there is no clear correlation between the solvent polarities and the molar extinction coefficients, in general polar solvents show lower values. As expected, the compound **3a** has blue shifted absorption at 468 nm in DCM as compared to **3b** at 490 nm in DCM (Fig. 5). The dye **3b** has $–NO_2$ group which is electron withdrawing and exhibits a red shifted absorption as it assists the azo group in pulling electrons and eventually shifts the absorption to the red region, whereas

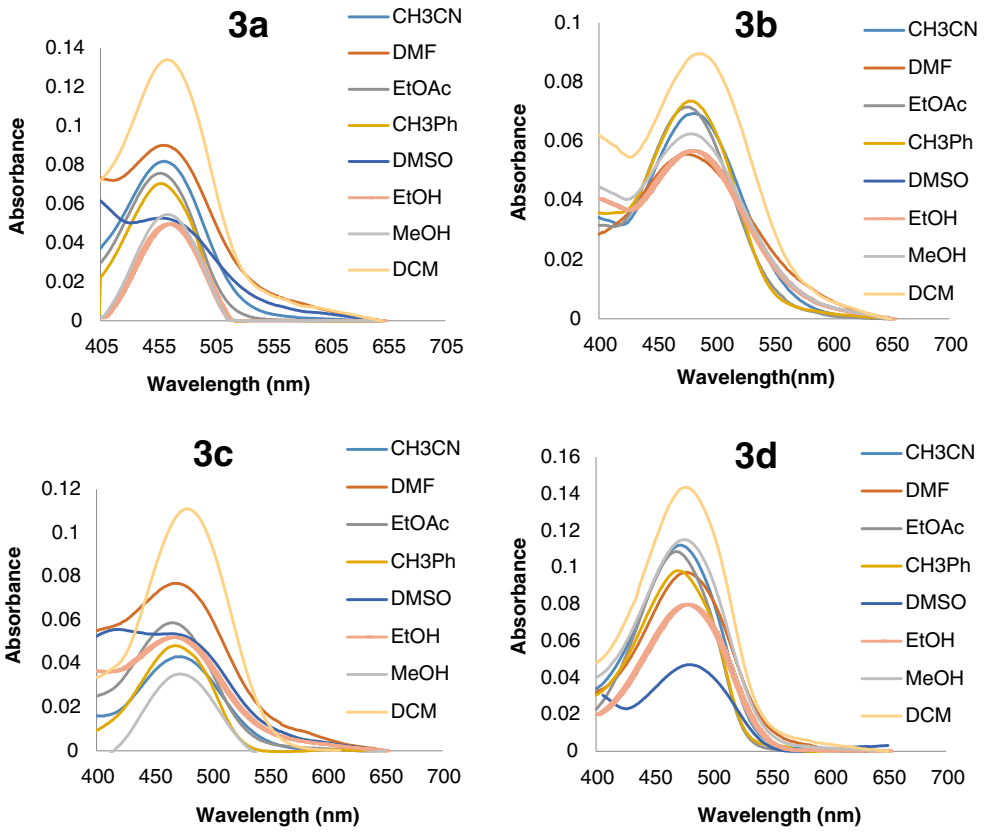

Fig. 5 Absorption spectra of compound **3a-3d** in various solvents

the compound **3c** with a –COOH group at *para*-position shows a red shift of 17 nm which is lower compared to the dye **3a**. Though the dye **3d** possesses an electron donating group (-OCH_3), it also has exhibited a red shift of 14 nm in absorption. The presence of electron withdrawing or donating group has induced a red shift in these compounds. The azo group (-N=N-), being an electron withdrawing can be involved in the charge transfer from both sides and hence enhances the red shifted absorption. This is also evident from FMO diagrams given in Table 5. The electron density at LUMO is mostly present on the azo group.

Though the absorption wavelengths of the dyes **3a-3d** are not solvent dependent, their fluorescence shows a greater impact of solvents. The emissions of all the dyes **3a-3d** ranges between 538 and 646 nm. The Stokes shift values are higher and are in the range of 2460–5662 cm^{-1} (68 to 166 nm) across the compounds in various solvents. The Stokes shifts are higher in polar solvents. The quantum yield values are on the lower side which are in the range of 0.0005 to 0.0210 (Table 1). The quantum yields are not uniform and are higher in non-polar solvents like toluene, dichloromethane and ethyl acetate (EtOAc) due to the lesser interaction with fluorophores as compared to the polar solvents. The order of the emission wavelength is dichloromethane>ethyl acetate>toluene amongst the non-polar solvents. The compounds have shown an unusual high Stokes shift, and may be attributed to the flexibility of the –N=N-Ar group at the 3-position which may be involved in vibrational relaxation at in the excited state lowering the energy of the emissive state (Fig. *6*).

The dyes **4a-4d**, which are the BF_2-complex derivatives of the dyes **3a-3d** absorb at a longer wavelength (~50–60 nm). The differences between the two kind chromophores are the rigidization of azo group and the presence of an electron deficient BF_2-core which has formed a more efficient acceptor in the case of dyes **4a-4d**. Though there is no significant effect of polarity on absorption wavelength but still has a marginal red shift in polar solvents (~15–20 nm). Among all, the dye **4b** is the most red shifted by ~20–40 nm as the nitro group is a strong withdrawer. The order of the substituents exhibiting longer wavelength is –H < $-OCH_3$ < −COOH < $-NO_2$. The fluorescence emission of 4a-4d exceeds 600 nm in all the solvents tested except for toluene in which their emission maxima is slightly lower than 600 nm. The fluorescence quantum yield has drastically improved in azo-BF2-complexes over the azo compounds, the order of the increase in quantum yield is about 10–100 folds. The quantum yields are the lowest in the $-NO_2$ substituted derivatives (**3b** and **4b**) in their respective series (Figs. 7 and 8).

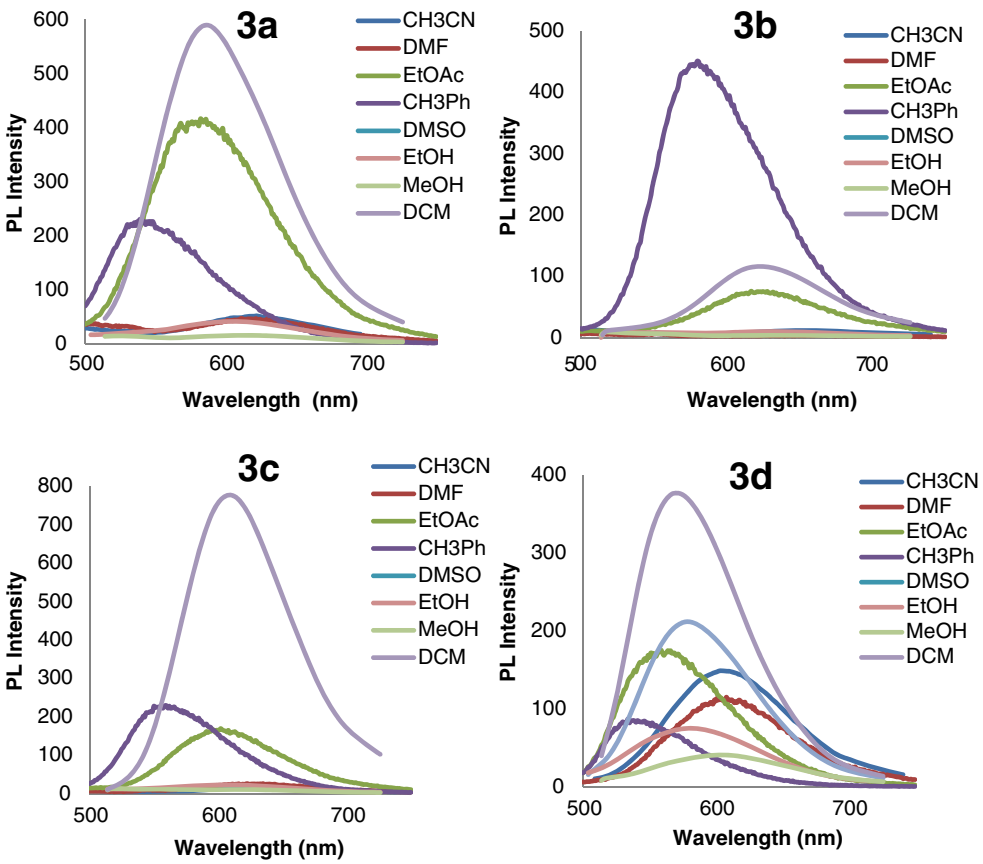

Fig. 6 Fluorescence emission spectra of compound **3a-3d** in various solvents

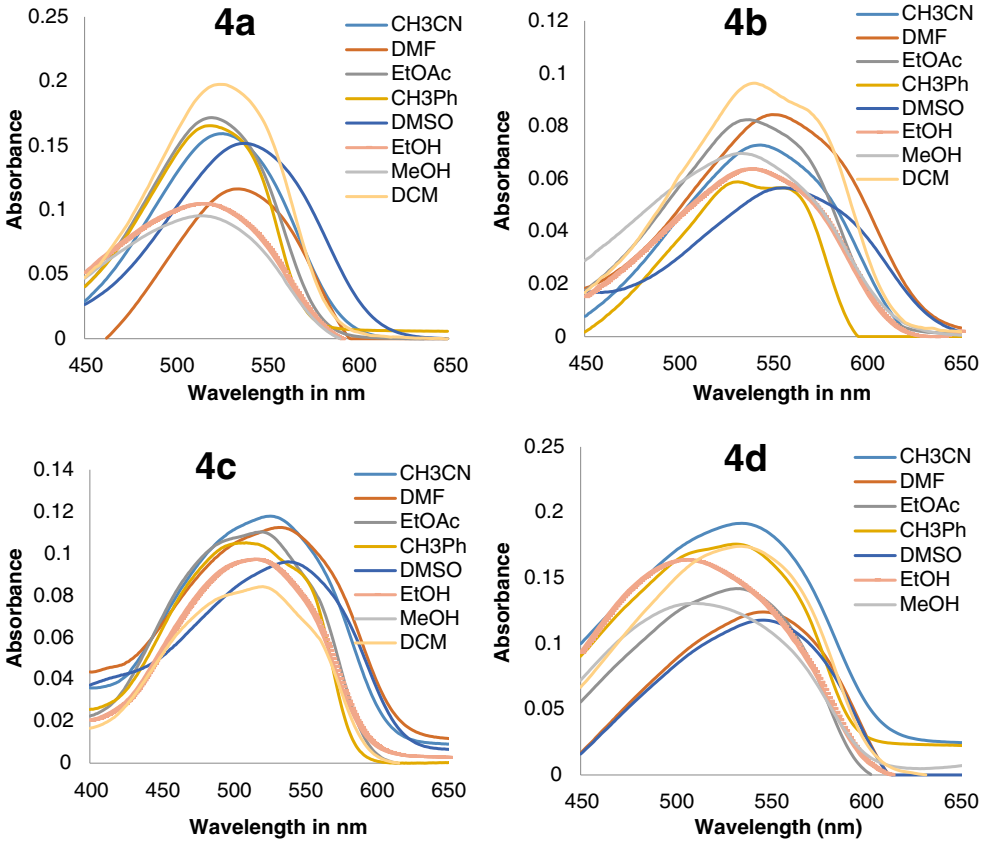

Fig. 7 Absorption spectra of compound **4a-4d** in various solvents

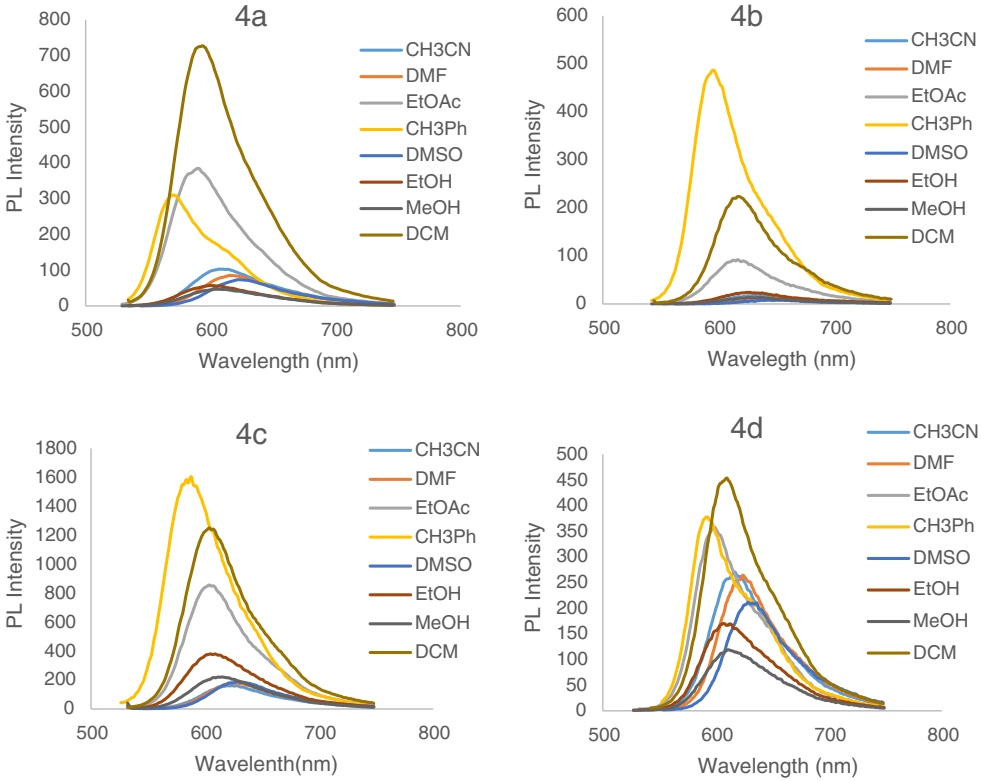

Fig. 8 Fluorescence emission spectra of compound **4a-4d** in various solvents

Table 2 Photophysical properties of compounds **4a-4d** and comparison with theoretical values

	Solvent	Experimental					Theoretical		
		λ_{abs} (nm)	f	λ_{em} (nm)	Stokes shift (cm^{-1})	Φ	Vertical excitation (nm)	f	Emission (nm)
4a	ACN	527	0.759	607	2501	0.0342	477	1.127	582
	DCM	528	0.487	592	2048	0.1902	478	1.132	608
	DMF	536	0.480	616	2423	0.0437	480	1.150	565
	DMSO	536	0.767	625	2657	0.0301	479	1.148	600
	EtOAc	521	0.782	586	2129	0.1106	475	1.106	566
	EtOH	520	0.535	600	2564	0.0311	477	1.130	562
	MeOH	517	0.487	605	2813	0.0258	476	1.122	583
	Tol	524	0.753	580	1843	0.0995	477	1.077	582
4b	ACN	546	0.378	633	2517	0.0126	500	1.255	569
	DCM	570	0.477	616	1310	0.1164	498	1.303	568
	DMF	557	0.438	650	2569	0.0081	504	1.284	574
	DMSO	554	0.271	650	2666	0.0086	503	1.279	618
	EtOAc	539	0.322	615	2293	0.0597	493	1.297	562
	EtOH	540	0.351	629	2620	0.0210	500	1.265	569
	MeOH	533	0.417	630	2889	0.0101	499	1.250	568
	Tol	559	0.417	597	1139	0.4175	487	1.363	557
4c	ACN	530	0.766	620	2739	0.071	480	1.315	550
	DCM	523	0.771	606	2619	0.8184	480	1.345	550
	DMF	541	0.647	627	2535	0.0943	483	1.340	554
	DMSO	535	0.602	631	2844	0.1162	483	1.336	554
	EtOAc	519	0.632	602	2657	0.3880	477	1.336	544
	EtOH	524	0.571	609	2664	0.2064	480	1.322	550
	MeOH	525	0.529	613	2734	0.1236	479	1.311	549
	Tol	518	0.529	595	2498	0.8845	476	1.374	540
4d	ACN	532	1.011	617	2590	0.0772	499	1.283	574
	DCM	534	0.670	608	2279	0.1407	501	1.297	576
	DMF	546	0.783	625	2315	0.1080	503	1.304	579
	DMSO	546	0.892	629	2417	0.1023	502	1.302	579
	EtOAc	525	0.636	600	2381	0.1141	498	1.281	572
	EtOH	505	0.948	609	3382	0.0543	500	1.287	574
	MeOH	519	0.801	613	2955	0.0448	499	1.278	573
	Tol	535	0.801	593	1828	0.1339	499	1.289	573

A comparison of the computed and experimental absorption and emission wavelengths for the dyes **3a-3d** and **4a-4d** are given in Tables 1 and 2 respectively. The deviations are higher for the compounds **4a-4d** with deviations ranging between 1.0 and 13.6 % in absorption, compared to 0.2 to 11.6 % deviation shown by the compounds **3a-3d** in absorption. A similar trend is followed in the emission calculations. The compounds **4a-4b**, which have a strong acceptor in the form of $–BF_2$ complex, makes the system different in its charge separation. The trends in solvatochromism exhibited by the molecules in the present study has been clearly demonstrated by the chosen computational method (Tables 1 and 2).

Solvent Polarity Function Plots

The solvatochromic behaviour of the dyes **3a-3d** and **4a-4d** was studied with the help of Lippert [31], Weller [32] and Rettig [32] plots. A complete account of the Lippert Mataga, Weller and Rettig equations are given in the supporting information.

The azo dye series **3a-3d** showed linear relation of Stokes shift with respect to the orientation polarizability function $f_1(\varepsilon, n)$ given by Lippert (Supporting information) plot and the correlation factors range between 0.43 and 0.86. while the corresponding boron complexes do not show any appreciable correlation (Supporting info). The linearity in the

photophysical behaviour of the dyes **3a-3d** suggest that the local excitation of the molecules is affected by the solvent polarity and the trend is more linear in polar aprotic and non-polar solvents. The molecules in polar protic solvents have shown more randomness in their photophysical properties, and is backed by the fact that H-bonding interactions of the protic solvents is not considered in this polarity function. The Weller's plot for the azo dyes (**3a-3d**) is linear leading to the inference that there is intra molecular charge transfer (ICT) affected by the solvent polarity. The flexibility around the azo group makes the ICT possible, and the molecule relaxes to a lower emissive state. This has been reflected in the higher stokes shifts of these molecules (Table 1)

On the other hand, the BF_2-complexes of the azo dyes i.e. **4a-4d** do not show any correlation with the solvent polarity. The plots of Stokes shift in cm^{-1} versus solvent polarity parameter $f_1(\varepsilon, n)$ (Lippert plot), emission in cm^{-1} versus solvent polarity parameter $f_2(\varepsilon, n)$ (Weller plot) and emission in cm^{-1} versus solvent polarity parameter $f_3(\varepsilon, n)$ (Rettig plot) were with very low regression coefficients. This implies that in the boron complexes due to rigidity the emissive state is not an ICT state but a local relaxed excited state. The lower (as compared to compound **3a-3d**) Stokes shift exhibited by the dyes in all the solvents adds to the justification. (Plots are given in supporting information.)

Dipole moment Ratio

The dyes **3a-3d** responds well to the solvent polarity functions $f(\varepsilon, n)$, the similar equations are introduced by Bilot-Kawski [33], Bakhshiev [34] and Liptay [35] for the estimation of the ratio of the excited state dipole moment and ground state dipole moment i.e. $\frac{\mu_e}{\mu_g}$. The equations are given in supporting information.

The dipole moments calculated with the above equations is tabulated in Table 3.

All the compounds show higher $\frac{\mu_e}{\mu_g}$ ratio suggesting a highly polar excited state. This leads to a positive solvatochromism. This observation is also supported by the red shifted absorption and emission spectrum in polar solvents. The Bilot-Kawski equation has consistently estimated lower $\frac{\mu_e}{\mu_g}$ ratio as compared to the Bakhshiev and Liptay Equations.

Table 3 Dipole moment ratio of compound 3a-3d by various methods

Method	3a	3b	3c	3d
Bilot-Kawski	4.297	4.372	5.317	4.519
Bakhshiev	4.629	4.871	6.267	5.026
Liptay	4.633	5.034	6.583	5.284

Transition Dipole Moment

In addition to the difference in dipole moments between the excited and ground states, the charge transfer character of the fluorophore can be understood from the oscillator strength (f) (Given in Tables 1 and 2 and transition dipole moment of the dyes (μ_{eg}). The effective number of electrons transition from the ground to excited state is usually described by the oscillator strength, which provides the absorption area in the electronic spectrum. The oscillator strength (f) can be calculated using the literature method [36]. Transition dipole moments for absorption (μ_{eg}) which is a measure of the probability of radiative transitions have been calculated for the dyes in different solvent environments [37]. The values of transition dipole moment (μ_{eg}) for the dyes in each solvent is given in Table 4.

The transition dipole moments calculated for all the dyes shows that higher transition dipole moment is observed for the BF_2-complexed azo dyes as compared to their azo anologues. The trend in solvent environment is not clear but broadly a higher transition dipole moment is observed in the polar solvents.

Frontier Molecular Orbitals

The FMO (Frontier Molecular Orbitals) involved in the electronic transition from $S_0 \rightarrow S_1$ are HOMO→LUMO in the dyes **3a-3d**. The electron density on the HOMO is located on the donor 7-N,N-diethylamino group and moves towards –N-NH-Ar group in the LUMO, and thus sets up a clear acceptor and donor relationship. The –nitro group in **3b** possess electron density in LUMO, and shows a higher degree of charge transfer resulting in a red shift in absorption.

The compounds **4a-4d** have similar donor (i.e. N, N-diethylamino group), but the LUMO shows electron density located on the BF_2-complexed core.

Table 4 Transition dipole moments (μ_{eg}) obtained from absorption properties of compound 3a-3d and 4a-4d in various solvents

Solvent	3a	3b	3c	3d	4a	4b	4c	4d
ACN	7.1	7.0	5.2	8.0	9.2	6.6	9.3	10.7
DCM	4.8	7.1	3.8	8.4	7.4	7.6	9.2	8.7
DMF	8.5	6.8	7.8	7.8	7.4	7.2	8.6	9.5
DMSO	6.8	5.8	7.0	5.4	9.3	5.6	8.3	10.2
EtOAc	6.4	6.9	6.0	7.6	9.3	6.1	8.3	8.4
EtOH	4.7	6.7	6.3	6.9	7.7	6.3	8.0	10.1
MeOH	4.9	7.1	6.8	8.4	7.3	6.9	7.7	9.4
Tol	5.8	7.0	5.1	7.4	9.1	7.0	7.6	9.5

Values expressed in Debye

NLO Properties

There are quite a few reports on the hyperpolarizability estimation of the coumarin molecules as they can be a good candidate for such applications [38–40]. The higher ratio of the excited state dipole moment and ground state dipole moment also suggests a higher charge transfer.

Calculation of α_{CT} from the Solvatochromic Data

The linear polarizability α_{CT} was evaluated experimentally for synthesized extended styryls. These values are obtained by two-level model using UV–vis absorption/emission spectroscopy. The solvatochromic method can also be utilized in the determination of dipole moment of the lowest lying charge transfer excited state [41]. All α_{CT} values are calculated for azo coumarins, which are compared with theoretically obtained α_{CT} or α_{xx} (Supporting information).

The dyes are expected to show good non-linear properties. There are various experimental and theoretical methods reported to evaluate β value. Theoretical methods to evaluate β value are based on the time-dependent perturbation theory [42, 43]. The common experimental methods used to obtain β values are the electric field induced second harmonic generation (EFISH) [44] and the hyper Rayleigh scattering (HRS) [45].

The methods described above lack the cost effectiveness and it demands a more elaborate experimental set up. The solvatochromic method is simple and cost effective and serves as an effective a priori approach in understanding the nonlinear optical behaviour of dyes.

The two level microscopic model to determine solvent dependent hyperpolarizability is based on Oudar equation [46, 47] which in modified form can be presented as,

$$\beta_{xxx} = \beta_{CT} = \frac{3}{2h^2c^2}\frac{v_{eg}^2\,\mu_{eg}^2\,\Delta\mu_{CT}}{\left(v_{eg}^2 - v_L^2\right)\left(v_{eg}^2 - 4v_L^2\right)} \quad (1)$$

where x the is the direction of charge transfer, h is Planck's constant (in erg × s), c is speed of light in vacuum (in cm s^{-1}), μ_{eg} is the transition dipole moment, v_L is the frequency of the reference incident radiation to which the β value would be referred, v_{eg} is the transition frequency and $\Delta\mu_{CT}$ is the difference between excited state and ground state dipole moment, the hyperpolarizability obtained by this equitation is the dominant component of the hyperpolarizability tensor β_{xxx} [48] and as the formula refers to charge transfer transition the hyperpolarizability obtained often indicated as β_{CT} (charge transfer). The $\Delta\mu_{CT}$ is obtained on the basis of McRae's theory [49, 50]

$$\overline{\vartheta}_{abs} - \overline{\vartheta}_{emn} = (\delta_{abs} + \delta_{emn}) + \frac{2\Delta\mu_{CT}^2}{hca^3}\left(\frac{\varepsilon-1}{\varepsilon+2} - \frac{n^2-1}{n^2+2}\right) \quad (2)$$

where $\overline{\vartheta}_{abs} - \overline{\vartheta}_{emn}$ is the Stokes shift (in cm^{-1}), δ_{abs} and δ_{emn} are the differences in the vibrational energy (in cm^{-1}) of the molecule in the excited and ground state for absorption and emission, respectively, a is the cavity radius within Onsager's model (in cm), ε is the relative dielectric constant and n^2 the static refractive index of the solvent. a was calculated by integration of the solvent accessible surface using density functional theory optimized geometry Eq. 2 can be written as,

$$\overline{\vartheta}_{abs} - \overline{\vartheta}_{emn} = \frac{2\Delta\mu_{CT}^2}{hca^3}\left(\frac{\varepsilon-1}{\varepsilon+2} - \frac{n^2-1}{n^2+2}\right) + (\delta_{abs} + \delta_{emn}) \quad (3)$$

Treating this Eq. 3 as,

$$y = mx + c \quad (4)$$

where, $y = \overline{\vartheta}_{abs} - \overline{\vartheta}_{emn}$, $m = m = \frac{2\Delta\mu_{CT}^2}{hca^3}$, $x = \left(\frac{\varepsilon-1}{\varepsilon+2} - \frac{n^2-1}{n^2+2}\right)$ and $c = (\delta_{abs} + \delta_{emn})$

Using the value of slope m, $\Delta\mu_{CT}$ was then derived, and the transition dipole moment μ_{eg}^2 is related to the oscillator strength f (Equation given in supporting information).

where, m is mass of electron, f is oscillator strength, $\overline{\vartheta}_{eg}$ is the absorption frequency in cm^{-1}, e is charge on electron. The oscillator strength can be obtained by integrated absorption coefficient of the absorption band.

The value of first hyperpolarizability obtained using the solvatochromic method is based on several assumptions and thus allow only approximate estimate of dominant tensor of total hyperpolarizability along the direction of charge transfer which is the major contributor to the total hyperpolarizability. Though the values are approximate it is possible to understand the trend in the hyperpolarizability values in a series of molecules (Table 5).

The BF_2-complexed molecules do not show prominent solvatochromism while the azo dyes (**3a-3d**) show. The experimental and calculated values of β_{xxx} for compounds **3a-3d** are given in Table 6.

The experimental and computed values of β_{xxx} for the dyes **3a** and **3d** are in good agreement. The compounds **3b** and **3c** having stronger electron withdrawing groups show appreciable difference between the experimental computational values of β_{xxx}.

The value of β_0 or total first order hyperpolarizability of the molecule gives an estimate of the NLO properties of the organic molecules. The computed values were compared with the values obtained for urea. The comparison of the values is given below in Table 7.

The total hyperpolarizability calculated is 46 to 1083 times greater than that of urea. The electron donating group (i.e.–OCH_3) in the dye **3d** contributes to the least total hyperpolarizability of the molecule. On the other hand the

Table 5 FMO (Frontier molecular orbital) for compound **3a-3d** and **4a-4d**

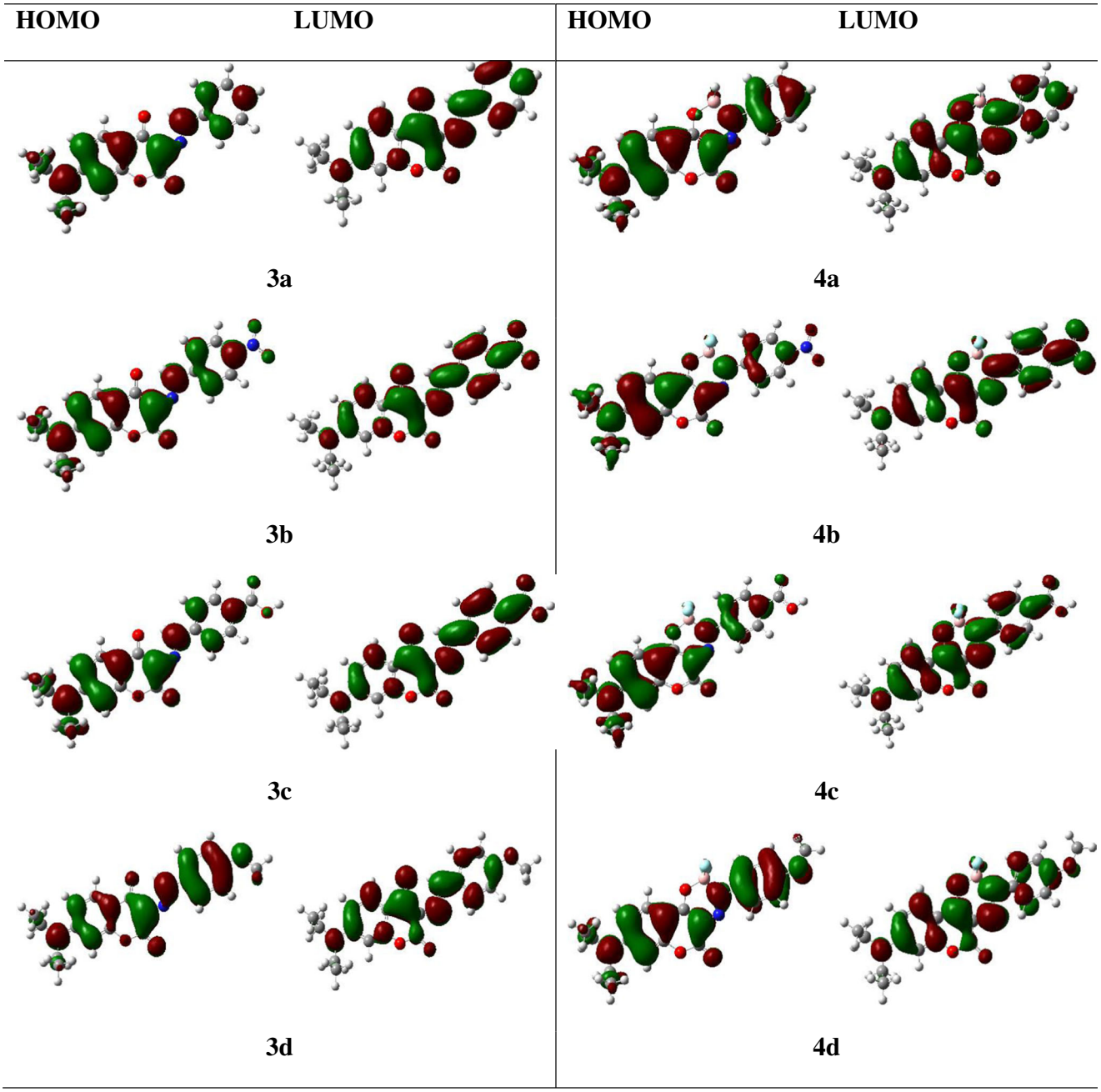

dye **3b** with electron withdrawing group shows 1083 times more value of hyperpolarizability than urea.

The second order hyperpolarizability ⟨γ⟩SD at molecular level originating from the electronic polarization in the non-resonant region can be treated by a three-level model [51–55]. The quasi-two-level model in place of three level model using the density matrix formalism leads to a simpler Eq. 5 [56, 57].

$$< \gamma > \propto \frac{1}{E_{eg}^{3}} \mu_{eg}^{2} \left(\Delta\mu^{2} - \Delta\mu_{eg}^{2} \right) \quad (5)$$

The value $\frac{1}{E_{eg}^{3}} \mu_{eg}^{2} \left(\Delta\mu^{2} - \Delta\mu_{eg}^{2} \right)$ is indicative of the value of second order hyperpolarizability and can be considered to be the "solvatochromic descriptor of second order hyperpolarizability" and the values calculated are given in supporting information.

The solvatochromic descriptor $<\gamma>$ of the second order hyperpolarizability of the compounds show higher values in the case of the dye **3d with** a strong donor i.e. –OCH3. The value for the dye **3b** remains to be the second highest. The electron flow enhancement in the azo core seems to be

Table 6 Linear polarizability α_{CT} calculated by solvatochromic method and computed α_{CT} for compound **3a-3d**

	3a		3b		3c		3d	
	$E\,\alpha_{xx}$	$C\,\alpha_{xx}$	$E\,\alpha_{xx}$	$C\,\alpha_{xx}$	$E\,\alpha_{xx}$	$C\,\alpha_{xx}$	$E\,\alpha_{xx}$	$C\,\alpha_{xx}$
ACN	1.73	4.07	1.78	2.29	0.96	2.27	2.31	4.43
DCM	0.74	3.88	1.72	2.18	0.50	2.16	2.39	4.23
DMF	2.34	4.07	1.54	2.29	2.03	2.27	2.04	4.43
DMSO	1.46	4.08	1.10	2.30	1.58	2.28	0.95	4.45
EA	1.39	3.77	1.65	2.12	1.25	2.11	2.00	4.12
EtOH	0.75	4.04	1.62	2.27	1.40	2.25	1.68	4.39
MeOH	0.84	4.06	1.82	2.28	0.52	2.27	2.54	4.42
Tol	1.05	3.42	1.60	1.94	0.81	1.94	1.75	3.73

$E\,\alpha_{xx}$ = Experimental $C\,\alpha_{xx}$ = Computational
Values are in the order of $\times 10^{-30}$ esu

enhancing the third order hyperpolarizability descriptor $<\gamma>$. The solvent effect is also evident on this parameter. Higher the polarity of the solvent, higher is the second order hyperpolarizability.

Computational γ Value (Second Order Static Hyperpolarizability)

The individual components of the second order static hyperpolarizability γ were obtained computationally. The values are considered to be proportional to the solvatochromic descriptor $<\gamma>$ of the second order hyperpolarizability. The values obtained are given in supporting information (Tables 8 and 9).

The values has a trend where higher polarity solvents show higher values of γ, but the similar trend is not followed by the solvatochromically obtained values.

Table 7 Expermental and computed β_{xxx} values for compound **3a-3d** in various solvents

Solvent	3a		3b		3c		3d	
	$E\,\beta_{xxx}$	$C\,\beta_{xxx}$	$E\,\beta_{xxx}$	$C\,\beta_{xxx}$	$E\,\beta_{xxx}$	$C\,\beta_{xxx}$	$E\,\beta_{xxx}$	$C\,\beta_{xxx}$
ACN	3.69	4.56	5.28	0.41	2.21	0.47	3.13	2.01
DCM	1.58	3.83	5.14	0.35	1.13	0.40	3.42	2.03
DMF	5.07	4.57	4.21	0.41	4.42	0.47	2.82	2.01
DMSO	3.14	4.63	3.04	0.41	3.67	0.47	1.35	2.01
EA	2.88	3.45	4.79	0.32	2.88	0.36	2.74	2.01
EtOH	1.62	4.44	4.68	0.40	3.10	0.45	2.38	2.02
MeOH	1.82	4.53	5.17	0.40	1.18	0.46	3.56	2.01
Tol	2.25	2.31	4.71	0.23	1.84	0.26	2.43	1.76

$E\,\beta_{xxx}$ =Experimental $C\,\beta_{xxx}$ = Computed
Values are in the order of $\times 10^{-30}$ esu

Table 8 Total first order hyperpolarizability calculated with B3LYP/6-31G (d) for compound **3a-3d**

	3a	3b	3c	3d
	β_o ($\times 10^{-30}$)			
ACN	134.88	447.01	254.14	20.12
DCM	115.27	384.05	220.90	14.03
DMF	135.19	447.99	254.65	20.22
DMSO	136.68	452.70	257.13	20.73
EA	104.83	350.05	202.86	11.34
EtOH	131.70	436.86	248.79	19.05
MeOH	134.18	444.78	252.97	19.88
Tol	72.02	240.86	144.05	11.12
Average	120.59	400.54	229.44	17.06
Ratio with urea (Urea: Compound)	326	1083	620	46

Conclusion

In conclusion, we have reported the fluorescent 3-azo coumarin compounds (**3a-3d**) with solvatochromism. The molecules were confirmed by spectral analysis like ^{1}HNMR, ^{13}CNMR, and mass spectra. A careful analysis of solvent polarity function and photophysical properties shows that there is presence of intra molecular charge transfer state (ICT) involved in the photo-excitation and emission of the molecules. There is a good linearity observed for dielectric constant and refractive index based solvent polarity functions like Lippert, Weller and Rettig functions. The dipole moment ratio calculated with different equations have revealed that there is a highly polar excited state involved in photoexcitations. The positive solvatochromism shown is attributed to this. On the other hand, the respective BF_2-complexes (**4a-4d**) which are the rigidized versions of the azocoumarins (**3a-3d**) do not show any linear relations with the solvent polarity parameters based on dielectric constant and refractive index. The locking of the flexible azo-group has restricted the ICT process and stokes shift is lowered, however there is a red shift observed in absorption as compared to the compound **3a-3d**. The overall hyperpolarizability compared with urea has 46 to 1083 times

Table 9 Second order static hyperpolarizability obtained computationally using B3LYP/6-31G(d) for **3a-3d**

Solvent	3a	3b	3c	3d
ACN	818	2339	1331	1082
DCM	690	1905	1126	920
DMF	820	2346	1334	1085
DMSO	830	2379	1350	1097
EA	622	1683	1018	834
EtOH	797	2267	1298	1056
MeOH	813	2323	1324	1077
Tol	414	1030	681	551

greater hyperpolarizability, and can be very good candidates as NLO materials. The second order static hyperpolarizability was found to be solvent dependent and reiterates the utility of these molecules as NLO materials.

Acknowledgments Abhinav Tathe is thankful to University Grants Commission, New Delhi (India) for award of Junior and Senior Research fellowships.

References

1. Cigáň M, Donovalová J, Szöcs V et al (2013) 7-(Dimethylamino)coumarin-3-carbaldehyde and its phenylsemicarbazone: TICT excited state modulation, fluorescent H-aggregates, and preferential solvation. J Phys Chem A 117: 4870–4883. doi:10.1021/jp402627a
2. Krzeszewski M, Vakuliuk O, Gryko DT (2013) Color-tunable fluorescent dyes based on benzo[c]coumarin. Eur J Org Chem 5631–5644. doi:10.1002/ejoc.201300374
3. Azzouz IM, Salah A (2012) Nonlinear optical absorption and NIR to blue conversion in highly stable polymeric dye rod. Appl Phys B 108:469–474. doi:10.1007/s00340-012-4915-y
4. Chen J, Liu W, Zhou B et al (2013) Coumarin- and rhodamine-fused deep red fluorescent dyes: synthesis, photophysical properties, and bioimaging in vitro. J Org Chem 78:6121–6130. doi:10.1021/jo400783x
5. Nedumpara RJ, Thomas KJ, Jayasree VK et al (2007) Study of solvent effect in laser emission from Coumarin 540 dye solution. Appl Opt 46:4786. doi:10.1364/AO.46.004786
6. Christie RM, Morgan KM, Islam MS (2008) Molecular design and synthesis of N-arylsulfonated coumarin fluorescent dyes and their application to textiles. Dye Pigment 76:741–747. doi:10.1016/j.dyepig.2007.01.018
7. Kim T-K, Lee D-N, Kim H-J (2008) Highly selective fluorescent sensor for homocysteine and cysteine. Tetrahedron Lett 49:4879–4881
8. Keskin SS, Aslan N, Bayrakçeken F (2009) Optical properties and chemical behavior of Laser-dye Coumarin-500 and the influence of atmospheric corona discharges. Spectrochim Acta A Mol Biomol Spectrosc 72:254–259. doi:10.1016/j.saa.2008.09.024
9. Painelli A, Terenziani F (2001) Linear and non-linear optical properties of push–pull chromophores: vibronic and solvation effects beyond perturbation theory. Synth Met 124:171–173. doi:10.1016/S0379-6779(01)00431-3
10. Jung HS, Kwon PS, Lee JWJHJY et al (2009) Coumarin-derived Cu(2+)-selective fluorescence sensor: synthesis, mechanisms, and applications in living cells. J Am Chem Soc 131:2008–2012. doi:10.1021/ja808611d
11. Sheng R, Wang P, Gao Y et al (2008) Colorimetric test kit for Cu2+ detection. Org Lett 10:5015–5018. doi:10.1021/ol802117p
12. Yazdanbakhsh MR, Ghanadzadeh A, Moradi E (2007) Synthesis of some new azo dyes derived from 4-hydroxy coumarin and spectrometric determination of their acidic dissociation constants. J Mol Liq 136:165–168. doi:10.1016/j.molliq.2007.03.005
13. Shahinian EGH, Haiduc I, Sebe I (2011) Synthesis and characterization of new azo coumarin dyes. UPB Sci Bull Ser B Chem Mater Sci 73:153–160
14. Morlet-Savary F, Ley C, Jacques P, Fouassier JP (2001) Photophysics of a bridged 7-diethylamino-4-methyl-coumarin C102: studying the hydrogen bonding effect by time resolved stimulated emission. J Phys Chem A 105:11026–11033
15. Griffiths J, Millar V, Bahra G (1995) The influence of chain length and electron acceptor residues in 3-substituted 7- N, N-diethylaminocoumarin dyes. Dye Pigment 28:327–339
16. Yang Y, Hughes RP, Aprahamian I (2012) Visible light switching of a BF2-coordinated azo compound. J Am Chem Soc 134:15221–15224. doi:10.1021/ja306030d
17. Li Y, Patrick BO, Dolphin D (2009) Near-Infrared absorbing azo dyes: synthesis and x-ray crystallographic and spectral characterization of monoazopyrroles, bisazopyrroles, and a boron-azopyrrole complex. J Org Chem 74:5237–5243. doi:10.1021/jo9003019
18. Kohn W, Sham LJ (1965) Self-consistent equations including exchange and correlation effects. Phys Rev 140:A1133–A1138. doi:10.1103/PhysRev.140.A1133
19. Menzel R, Ogermann D, Kupfer S et al (2012) 4-Methoxy-1,3-thiazole based donor-acceptor dyes: characterization, X-ray structure, DFT calculations and test as sensitizers for DSSC. Dye Pigment 94:512–524. doi:10.1016/j.dyepig.2012.02.014
20. Lee C, Yang W, Parr RG (1988) Development of the Colle-Salvetti correlation-energy formula into a functional of the electron density. Phys Rev B 37:785–789. doi:10.1103/PhysRevB.37.785
21. Tablet C, Minea L, Dumitrache L, Hillebrand M (2012) Experimental and theoretical study of the inclusion complexes of 3-carboxycoumarin acid with β- and 2-hydroxypropyl-β-cyclodextrins. Spectrochim Acta A Mol Biomol Spectrosc 92:56–63. doi:10.1016/j.saa.2012.02.027
22. Rajeev S, Husain MM (2011) Solvent effect on coumarin dye: calculation of ground and excited state dipole moments. J Indian Chem Soc 88:1541–1546
23. Deshmukh MS, Sekar N (2014) A combined experimental and TD-DFT investigation of three disperse azo dyes having the nitroterephthalate skeleton. Dye Pigment 103:25–33. doi:10.1016/j.dyepig.2013.10.035
24. Wong MW, Frisch MJ, Wiberg KB (1991) Solvent effects. 1. The mediation of electrostatic effects by solvents. J Am Chem Soc 113: 4776–4782. doi:10.1021/ja00013a010
25. Frisch MJ, Trucks GW, Schlegel HB et al (2009) Gaussian 09, revision C.01. Gaussian 09, revis. B.01. Gaussian, Inc, Wallingford
26. Dennington R, Keith TMJ (2009) Gaussview
27. Knierzinger A, Wolfbeis OS (1980) Syntheses of fluorescent dyes. IX. New 4-hydroxycoumarins, 4-hydroxy-2-quinolones, 2H,5H-Pyrano[3,2-c]benzopyran-2,5-diones and 2H,5H-Pyrano[3,2-c]quinoline-2,5-diones. J Heterocycl Chem 17:225–229. doi:10.1002/jhet.5570170204
28. Ozen AS, Doruker P, Aviyente V (2007) Effect of cooperative hydrogen bonding in azo-hydrazone tautomerism of azo dyes. J Phys Chem A 111:13506–13514. doi:10.1021/jp0755645
29. Qu J, Liu B, He J (2014) Photofading mechanisms of azo dye in its azo and hydrazone forms under UV irradiation. J Chem Pharm Res 6:1149–1154
30. Umape PG, Patil VS, Padalkar VS et al (2013) Synthesis and characterization of novel yellow azo dyes from 2-morpholin-4-yl-1,3-thiazol-4(5H)-one and study of their azo–hydrazone tautomerism. Dye Pigment 99:291–298. doi:10.1016/j.dyepig.2013.05.002
31. Lippert E (1957) Spektroskopische Bestimmung des Dipolmomentes aromatischer Verbindungen im ersten angeregten Singulettzustand. Z Elektrochem Ber Bunsenges Phys Chem 61: 962–975. doi:10.1002/bbpc.19570610819
32. Valeur B (2001) Molecular fluorescence. doi:10.1002/3527600248
33. Bilot L, Kawski A (1962) Zur Theorie des Einflusses von Lösungsmitteln auf die Elektronenspektren der Moleküle. Zeitschrift Naturforsch. Tl. A 17
34. Bakhshiev NG (1972) Spectroscopy of intermolecular interactions (in Russian). Isd. Nauka, Leningrad
35. Liptay W (1965) Die Lösungsmittelabhängigkeit der Wellenzahl von Elektronenbanden und die chemisch-physikalischen Grundlagen. Z Naturforsch A 20a:1441–1447

36. Turro NJ (1978) Modern molecular photochemistry. Benjamin-Cummings, New York
37. Coe BJ, Harris JA, Asselberghs I et al (2002) Quadratic nonlinear optical properties ofN-Aryl stilbazolium dyes. Adv Funct Mater 12: 110–116. doi:10.1002/1616-3028(20020201)12:2<110::AID-ADFM110>3.0.CO;2-Y
38. Sharafudeen KN, Adithya A, Vijayakumar S et al (2011) Multiphoton absorption process and self-focusing effect in coumarin derivative doped PMMA films by Z-scan and optical limiting studies. Curr Appl Phys 11:1089–1093. doi:10.1016/j.cap.2011.02.001
39. Sun YF, Wang HP, Chen ZY, Duan WZ (2013) Solid-state fluorescence emission and second-order nonlinear optical properties of coumarin-based fluorophores. J Fluoresc 23:123–130. doi:10.1007/s10895-012-1125-2
40. Raj RK, Gunasekaran S, Gnanasambandan T, Seshadri S (2015) Combined spectroscopic and DFT studies on 6-bromo-4-chloro-3-formyl coumarin. Spectrochim Acta A Mol Biomol Spectrosc 139: 505–514. doi:10.1016/j.saa.2014.12.024
41. Abbotto A, Beverina L, Bradamante S et al (2003) A distinctive example of the cooperative interplay of structure and environment in tuning of intramolecular charge transfer in second-order nonlinear optical chromophores. Chem - A Eur J 9:1991–2007. doi:10.1002/chem.200204356
42. Oudar JL, Zyss J (1982) Structural dependence of nonlinear-optical properties of methyl-(2,4-dinitrophenyl)-aminopropanoate crystals. Phys Rev A 26:2016–2027. doi:10.1103/PhysRevA.26.2016
43. Morley JO, Docherty VJ, Pugh D (1987) Non-linear optical properties of organic molecules. Part 2. Effect of conjugation length and molecular volume on the calculated hyperpolarisabilities of polyphenyls and polyenes. J Chem Soc Perkin Trans 2:1351. doi:10.1039/p29870001351
44. Meshulam G, Kotler Z, Berkovic G (2002) Time-resolved electric-field-induced second harmonic: simultaneous measurement of first and second molecular hyperpolarizabilities. Opt Lett 27:1132–1134. doi:10.1364/OL.27.001132
45. Heesink GJT, Ruiter AGT, Van Hulst NF, Bölger B (1993) Determination of hyperpolarizability tensor components by depolarized hyper Rayleigh scattering. Phys Rev Lett 71:999–1002. doi:10.1103/PhysRevLett.71.999
46. Oudar JL, Chemla DS (1977) Hyperpolarizabilities of the nitroanilines and their relations to the excited state dipole moment. J Chem Phys 66:2664. doi:10.1063/1.434213
47. Carlotti B, Flamini R, Kikaš I et al (2012) Intramolecular charge transfer, solvatochromism and hyperpolarizability of compounds bearing ethenylene or ethynylene bridges. Chem Phys 407:9–19. doi:10.1016/j.chemphys.2012.08.006
48. Paley MS, Harris JM, Looser H et al (1989) A solvatochromic method for determining second-order polarizabilities of organic molecules. J Org Chem 54:3774–3778. doi:10.1021/jo00277a007
49. McRae EG (1957) Theory of solvent effects on molecular electronic spectra. Frequency shifts. J Phys Chem 61:562–572. doi:10.1021/j150551a012
50. Bruni S, Cariati E, Cariati F et al (2001) Determination of the quadratic hyperpolarizability of trans-4-[4-(dimethylamino)styryl]pyridine and 5-dimethylamino-1,10-phenanthroline from solvatochromism of absorption and fluorescence spectra: a comparison with the electric-field-induced second-harmon. Spectrochim Acta A Mol Biomol Spectrosc 57: 1417–1426. doi:10.1016/S1386-1425(00)00483-2
51. Oudar JL (1977) Optical nonlinearities of conjugated molecules. Stilbene derivatives and highly polar aromatic compounds. J Chem Phys 67:446–457. doi:10.1063/1.434888
52. De Paris R (1982) Nonlinear-optical properties. Phys Rev A 26: 2016–2027
53. Kwon OP, Jazbinsek M, Seo JI et al (2010) First hyperpolarizability orientation in asymmetric pyrrole-based polyene chromophores. Dye Pigment 85:162–170. doi:10.1016/j.dyepig.2009.10.019
54. Weaver CS, Smith SW, Hyndman RD et al (1991) + 0.028. Science 252:103–106
55. Cheng L-T, Tam W, Stevenson SH et al (1991) Experimental investigations of organic molecular nonlinear optical polarizabilities. 1. Methods and results on benzene and stilbene derivatives. J Phys Chem 95:10631–10643. doi:10.1021/j100179a026
56. Dirk CW, Cheng L-T, Kuzyk MG (1992) A simplified three-level model describing the molecular third-order nonlinear optical susceptibility. Int J Quantum Chem 43:27–36. doi:10.1002/qua.560430106
57. Kuzyk MG, Dirk CW (1990) Effects of centrosymmetry on the nonresonant electronic third-order nonlinear optical susceptibility. Phys Rev A 41:5098–5109. doi:10.1103/PhysRevA.41.5098